

Role of organic phosphates and phosphonates in catalysing dynamic exchange reactions in thiol-click vitrimers

*Khadijeh Moazzen, Elisabeth Rossegger, Walter Alabiso, Usman Shaukat and Sandra Schlögl**

K. Moazzen, E. Rossegger, W. Alabiso, U. Shaukat, Dr. S. Schlögl
Polymer Competence Center Leoben GmbH, Roseggerstrasse 12, 8700 Leoben, Austria
E-mail: sandra.schloegl@pccl.at

Keywords: catalyst, organic phosphates, organic phosphonates, thermo-activated transesterification, vitrimers

Owing to their strong Brønsted acidity, organic phosphates and phosphonates are able to catalyse dynamic transesterification reactions in hydroxyl ester networks. Compared to commonly used transesterification catalysts, they are highly soluble in a wide range of acrylate monomers and neither affect cure kinetics nor shelf-life of photocurable acrylate and thiol-acrylate resins. Additionally, they promote fast stress relaxation and, by using derivatives with functional groups, can be covalently incorporated within the photopolymer network. These salient features make organic phosphates and phosphonates ideal catalysts for the design and processing of photoreactive vitrimers. Herein, the catalytic activity of selected methacrylate-functional phosphates and vinyl-functional phosphonates on dynamic transesterifications are studied in a comprehensive way. They are incorporated in a low-T_g thiol-acrylate photopolymer providing functional –OH and ester moieties. Cure kinetics and thermo-mechanical properties are not significantly affected by the structure and functionality of the catalyst. In contrast, time-dependent stress relaxation measurements clearly show that relaxation time and activation energy correlate well with the pK_a value of the Brønsted acids. The better understanding of the role of organic phosphates and phosphonates expands the scope of transesterification catalysts and is particularly interesting for the design of photoreactive vitrimers, which can be additively manufactured by using vat polymerisation techniques.

1. Introduction

Dynamic covalent bonds impart unique features such as self-healability, recyclability, malleability and shape memory into polymer networks.^[1] Whilst the concept of dynamic covalent bonds can be realized by numerous reversible reaction pathways, the most intensively-studied and widely-applied one relies on the thermo-activated transesterification of hydroxyl ester moieties.^[2] In particular, the pioneering work of Leibler et al. on malleable epoxy-based networks has become the starting point for exploiting transesterifications in the design of functional polymers.^[3] Dynamic networks based on thermo-activated transesterifications are associative in nature and maintain their network connectivity at elevated temperature.^[4] The thermally-induced bond breakage and reformation reactions occur simultaneously and influence the viscoelastic properties of the dynamic networks at elevated temperature. Below the so-called topology freezing transition temperature (T_v), the exchange reactions are slow and the network properties are comparable to a classic thermoset. Above T_v , the exchange reactions are accelerated and the related topological rearrangements induce a viscoelastic flow of the network, which follows an Arrhenius trend.^[3] Since vitreous silica shows a similar behavior, this new class of dynamic polymer networks was termed vitrimers. To enhance the exchange rate of thermo-activated transesterifications, catalysts are typically employed.^[5, 6] The selection of the catalyst is guided by parameters such as the catalyst's (in)solubility, temperature stability and activity as well as long-term performance such as catalyst ageing or leaching.^[7] Further considerations include undesirable catalyst migration, which has been addressed either by covalent attachment of the catalyst to the network^[8] or the usage of polymeric catalysts.^[9]

The most frequently-used transesterification catalysts for vitrimers are organic zinc salts such as zinc acetate and zinc acetylacetonate, which activate the ester group by increasing its electrophilicity via polarization. In the presence of these Lewis acids, the reactive species are brought together through coordination bonds and the alcohol/alkoxide equilibrium is shifted

towards higher nucleophilic alkoxide.^[10] Apart from the classical epoxy-acid vitrimer of Leibler et al.,^[5] organic zinc salts have been applied in numerous vitrimer systems such as composites from epoxidized natural rubber (ENR) cross-linked with either carboxyl group-functionalised carbon nanodots^[11] or cellulose nanocrystals.^[12] Other groups introduced $\text{Zn}(\text{OAc})_2$ in silica-epoxy composites from diglycidyl ether of bisphenol A (DGEBA) and fatty acids^[13] or in ENR-dodecanedioic acid networks.^[14] Advancing from thermally-cured networks, Zhang and co-workers used $\text{Zn}(\text{OAc})_2$ to catalyse transesterifications in photocurable acrylate systems.^[15] They reported that the dynamic acrylate photopolymers were able to rapidly relax stresses at 180 °C, and subsequently, demonstrated a thermo-activated healing and re-shaping of 3D printed structures. However, the network design is limited as $\text{Zn}(\text{OAc})_2$ is insoluble in commonly used acrylate monomers.

Other prominent types of transesterification catalysts are organic bases such as the guanidine base 1,5,7-triazabicyclo[4.4.0]dec-5-ene (TBD), whose catalytic activity relies on an enhancement of the nucleophilicity of the –OH moieties by H-bonding. TBD was shown to be an effective transesterification catalyst in composites from DGEBA and adipic acid filled with carbon nanotubes^[16] or in epoxy-based composites containing graphene.^[17] Recently, we have demonstrated that TBD also catalyses transesterification reactions in hydrogenated and carboxylated nitrile butadiene rubber crosslinked with either bi-functional epoxides or epoxy-functionalized inorganic filler.^[18] Although Bowman and co-workers successfully applied TBD for the preparation of dynamic thiol-ene networks, the catalyst suffers from several drawbacks when it comes to the processing and 3D printing of photocurable vitrimers.^[19] On the one hand, it acts as radical scavenger and retards radically induced photopolymerisation reactions. On the other hand, it catalyses the thiol-Michael reaction in thiol-click resins, which leads to an immediate gelation of the resins.^[20]

Along with the basic-catalysed mechanism, the transesterification in vitrimers is also accelerated in the presence of Brønsted acids. In acid-catalysed transesterifications, the

electrophilicity of the carbonyl ester group is increased by protonation, which makes the carbonyl group more susceptible to a nucleophilic attack. A tetrahedral intermediate is formed by reaction with an –OH group in the network yielding a new ester bond by subsequent proton transfer, departure of the leaving group and deprotonation.^[21] Bates et al. studied the Brønsted acid-catalysed transesterification in hydroxyl-functional polyesters and applied strong protic acids with a pKa varying between -12 (triflic acid) and 0.81 (trichloroacetic acid).^[22] They observed a distinctive stress relaxation, which increased with decreasing pKa value of the acid catalyst.

Recently, we have demonstrated the acid-catalysed transesterification in thiol-acrylate photopolymers by using phosphate monoesters as strong Brønsted acids.^[20] Whilst mineral phosphates have been widely applied in the heterogeneous catalysis of transesterifications in solution,^[23] we could show the catalytic activity of organic counterparts in solid polymer networks. Organic phosphates are ideal catalyst for developing photocurable vitrimers as they are not compromising on shelf-life or cure kinetics of photocurable acrylate and thiol-ene systems. In addition, due to their high solubility in a wide range of acrylate monomers they enable a facile tailoring of mechanical and thermal properties of vitrimers.

2. Results and Discussion

To get a better understanding of the catalytic activity of organic phosphates and phosphonates in photocurable vitrimers, we studied the performance of selected derivatives with varying logarithmic acid dissociation constants (pKa) (Figure 1a). The pKa values were taken from literature and were referenced in H₂O. It should be noted that they are dependent on the medium/solvent in which they are measured, as they describe the thermodynamic equilibrium between a selected Brønsted acid and its conjugate base plus a proton.^[24] When it comes to solid polyester vitrimers, Bates and co-workers proposed that the absolute pKa values might change but the relative trend should still hold.^[22]

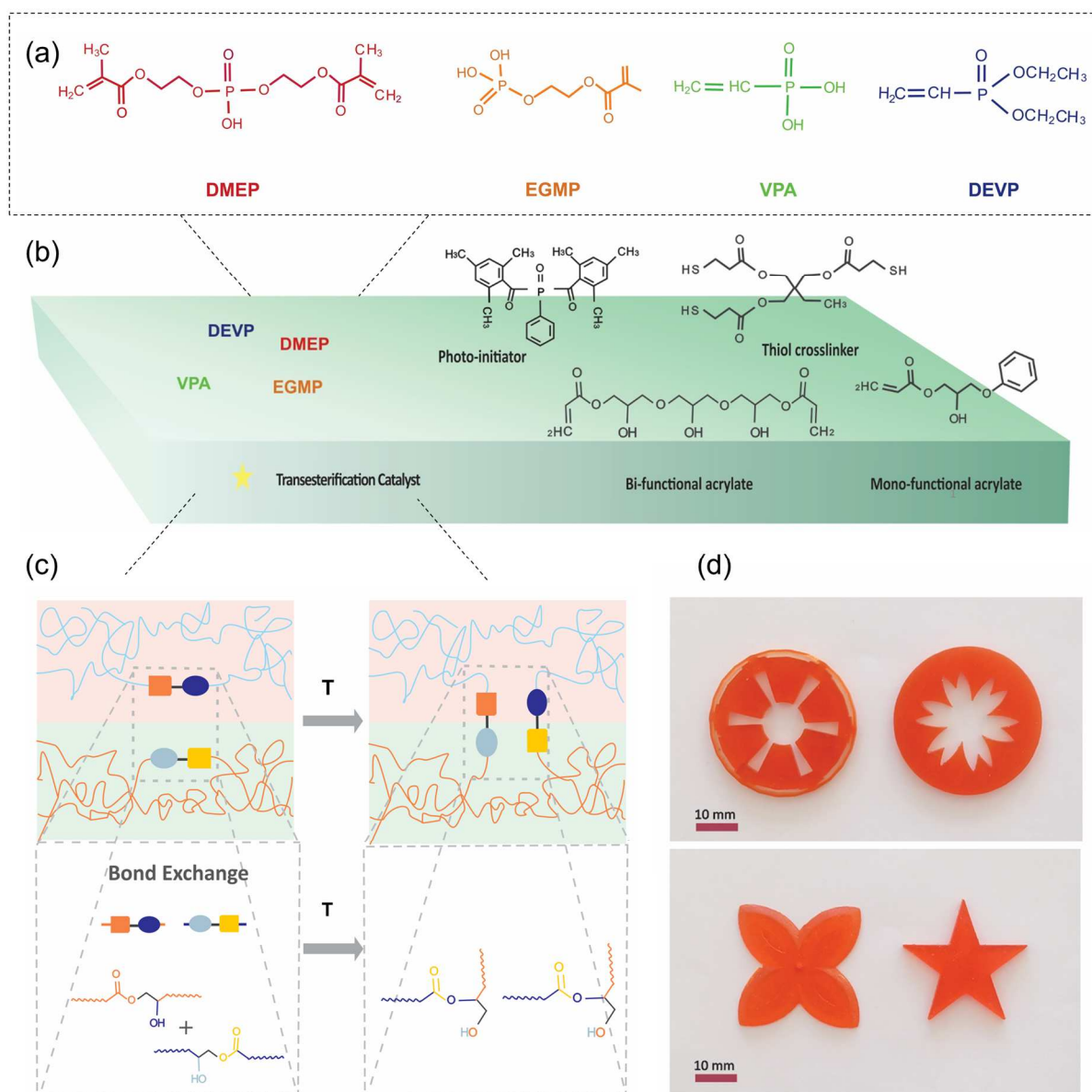


Figure 1. (a) Organic phosphates and phosphonates used as transesterification catalysts in thiol-acrylate vitrimers. (b) Photocurable monomers, crosslinker and photoinitiator used for the preparation of the thiol-acrylate matrix. (c) Schematic representation of dynamic exchange reactions in thiol-acrylate vitrimers relying on thermo-activated transesterifications. (d) DLP 3D printed test structures.

For this study, we selected ethylene glycol methacrylate phosphate (EGMP) and bis (2-methacryloyloxy)ethyl phosphate (DMEP), which are typically applied as corrosion inhibitors in polymeric coatings.^[25] DMEP has a pKa value of 1.7,^[26] whilst the pKa of EGMP amounts to 2.15.^[27] Moreover, EGMP and DMEP bear methacrylate functions, through which they can be covalently incorporated into a photopolymer network.

Along with phosphates, we employed weaker organic phosphonates including vinyl phosphonic acid (VPA) and diethyl vinyl phosphonate (DEVP), which are popular precursors for functional polymers used in fuel cells or polyelectrolytic membranes.^[28] Moreover, they comprise a terminal vinyl group for covalent attachment to the photopolymer network. Whilst VPA has a pKa value of 2.74^[29] DEVP does not contain any free –OH groups, and it is a very weak acid. For DEVP, there were no pKa data available in literature, but we assume it is well above 20, as diethyl phenyl phosphonate has a pKa of 27.6.^[30]

The catalysts were added to a photocurable thiol-acrylate formulation containing 50 mol% 2-hydroxy-3-phenoxy propyl acrylate, 25 mol% glycerol 1,3-diglycerolate diacrylate, 25 mol% trimethylolpropane tri(3-mercaptopropionate) and 2 wt% phenylbis(2,4,6-trimethylbenzoyl)phosphine oxide as photoinitiator (Figure 1b). Light triggered curing of the formulation yielded a thiol-acrylate photopolymer with ample –OH and carbonyl groups, which are able to undergo dynamic exchange reactions in the presence of an appropriate transesterification catalyst (Figure 1c). For a direct comparison of the catalytic activity, the catalyst content was kept constant at 3.75 mol (related to the free –OH groups in the network). As the kinetics of dynamic exchange reactions is also governed by the network's chain mobility and crosslink density, we determined cure kinetics, crosslink density and thermo-mechanical properties of the thiol-acrylate network as a function of the applied catalyst.^[7, 31] In the first step, the photo-induced cure kinetics of the catalysed formulations was monitored by FTIR spectroscopy and compared with a non-catalysed one (FTIR spectra of a DMEP catalysed network are provided as an example in Figure S1 in supporting information). Figure 2a provides the time-dependent depletion of the characteristic absorption bands of acrylate (1635 cm^{-1}) and thiol groups (2570 cm^{-1}). Both catalysed and non-catalysed thiol-acrylate formulations show a comparable cure rate and final conversion of the monomers is obtained upon 2 minutes UV exposure. The final acrylate conversion ranges between 80 and 83%, whilst the thiol conversion does not exceed 53%. The higher acrylate conversion is explained

by the mixed-mode chain growth/step growth-like photopolymerisation mechanism of the radical-mediated thiol-acrylate reaction. Due to their electron-withdrawing groups, acrylates exhibit a lower reactivity in thiol-ene reactions than electron-rich alkenes.^[32]

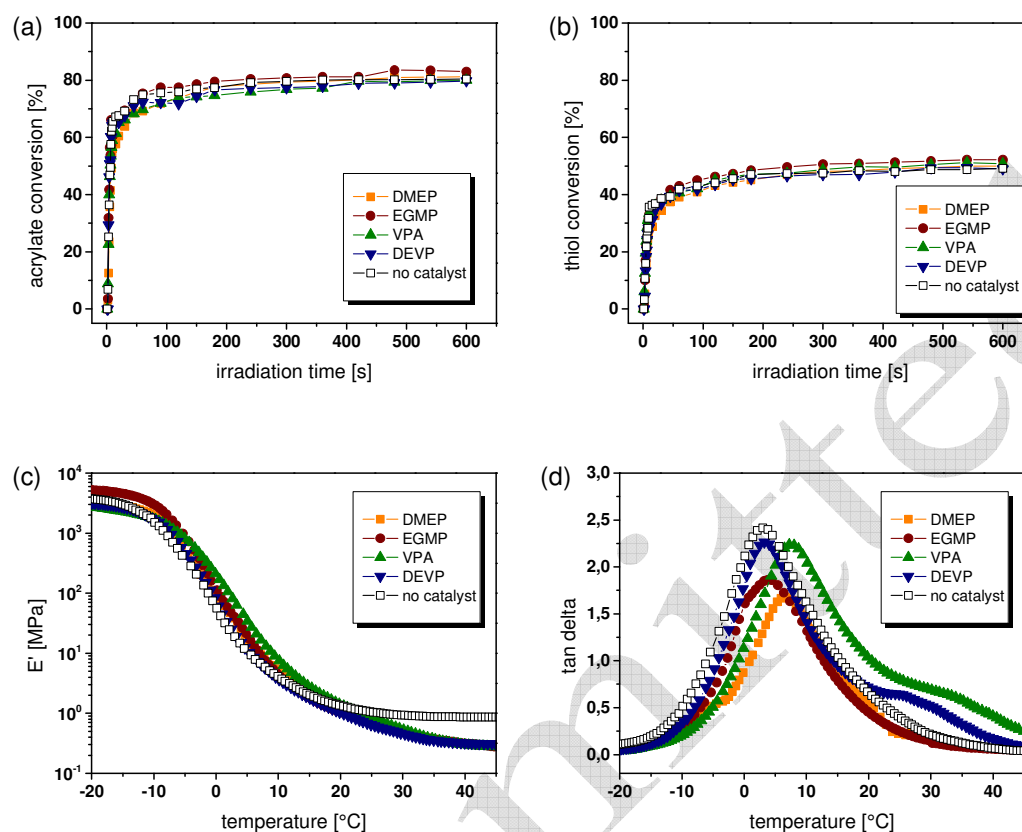


Figure 2. Following the cure kinetics in catalysed and non-catalysed thiol-acrylate formulations by FTIR spectroscopy. The normalized peak area of the IR absorption bands of the (a) acrylate groups (1635 cm^{-1}) and (b) thiol groups (2570 cm^{-1}) is plotted against exposure time. Irradiation ($\lambda = 420 - 450\text{ nm}$, 3.3 mW cm^{-2}) was performed under air. The lines are a guide for the eye. (c) Storage modulus and (d) tan delta curves of cured thiol-acrylate formulations as a function of temperature, plotted for various transesterification catalysts.

Consequently, the acrylate radicals are not only participating in chain transfer reactions but also in propagation reactions, yielding heterogeneous networks with intertwined thiol-ene and homopolymerised acrylate segments.^[33]

The broad tan delta curves obtained from dynamic mechanical analysis (DMA) confirm the heterogeneous network structure of the investigated thiol-acrylate networks (Figure 2d).

Whilst the cure kinetics showed a comparable final monomer conversion of the networks under investigation, the DMA data reveal that the networks slightly differ in their network heterogeneity. The glass transition region ranges from -15 to 45 °C, showing its maximum of tan delta between 3 and 8 °C. With a storage modulus of 0.8 – 1.5 MPa at 20 °C (Figure 2c), the networks are flexible but reasonably stiff to produce free-standing objects. Together with the fast cure speed and the high storage stability of the resins, these features enable a facile 3D printing of polymeric structures via digital light processing (DLP) (Figure 1d). To determine the crosslinking density of the catalysed and non-catalysed thiol-acrylate systems, equilibrium swelling measurements were conducted in dichloromethane. For sample preparation, discs with a diameter of 10 mm were DLP 3D printed (Table 1). The gel content varies between 63.5 ± 2.1 and 70.4 ± 1.4 %, is slightly higher for catalysed networks and decreases with increasing acidity of the catalyst.

Table 1. Properties of catalysed and non-catalysed thiol-acrylate networks

| catalyst | E' at 20 °C [MPa] | T_g [°C] | T_v [°C] | mass swelling ratio | gel content [%] |
|----------------|------------------------|---------------|---------------|---------------------|--------------------|
| without | 1.03 | 3 | - | 17.8 ± 1.5 | 63.5 ± 2.1 |
| DEVP | 0.98 | 3 | 49 | 16.5 ± 0.3 | 64.6 ± 1.3 |
| VPA | 1.32 | 8 | 50 | 14.5 ± 0.4 | 66.2 ± 1.3 |
| EGMP | 1.30 | 4 | 55 | 13.1 ± 0.6 | 67.4 ± 2.2 |
| DMEP | 1.25 | 7 | 59 | 12.7 ± 1.6 | 70.4 ± 1.4 |

In general, the low gel content can be explained by residual acrylate monomers as well as thiol crosslinker, which have not been incorporated within the photopolymer during the curing reaction and are extracted from the swollen networks. However, the increasing gel content indicates a higher crosslink density of the related networks. This is also confirmed by the

mass swelling ratios, which gradually decrease from non-catalysed to DMEP catalysed networks. The rising crosslinking density might be explained by acid-catalysed thiol-ene reactions, which proceed during storage of the cured samples under dark conditions.^[34] We observed acid-catalysed dark reactions of the thiol-acrylate resin at higher catalyst contents. Whilst at 3.75 mol%, the resin is stable over more than one week, a premature gelation occurs within 24 h if the catalyst content is exceeding 15 mol%. To confirm the occurrence of post-curing reactions, we studied the progress of the acrylate and thiol conversion of the DMEP catalysed network under dark conditions. For this, the network was irradiated until reaching maximum final monomer conversion and then stored at room temperature for 24 h. The data clearly reveal a further increase of the acrylate (from 81 to 84%) and thiol conversion (from 53 to 56%) upon prolonged storage at room temperature. From the results it can be concluded that the employed organic phosphates and phosphonates do not compromise on the photocure kinetics but induce acid-catalysed dark reactions, which increase the crosslink density of the catalysed thiol-acrylate networks.

The catalytic activity of the compounds was compared in subsequent temperature-dependent stress relaxation studies. For sample preparation, discs with a diameter of 10 mm were printed with DLP 3D printing. The stress relaxation of the networks was measured between 140 and 200 °C. Under the applied conditions, the chain segments of the low-T_g networks are highly mobile and facilitate bond exchange reactions. Figure 3a shows the time-dependent evolution of the relaxation modulus at 180 °C for non-catalysed as well as catalysed thiol-acrylate systems (Figure 3a). As reported in previous work, the thiol-acrylate network exhibits a slight stress relaxation, even in the absence of a transesterification catalyst.^[20] This is attributed to a thermal release of volumetric shrinkage stresses arising during network evolution.^[35]

In the presence of the protic Brønsted acids DMEP, EGMP and VPA, a fast relaxation is observed, whose reaction rate increases with decreasing pK_a value. Even at a higher crosslinking degree, the DMEP catalysed network only requires 15 min to relax 63% of the

initial stress. In contrast, the lower crosslinked VPA catalysed network needs 62 min under the same conditions. From the results it is concluded that the exchange rate is mainly governed by the acidity of the catalyst, whilst the crosslink density (at least in the investigated range of the networks) plays a minor role.

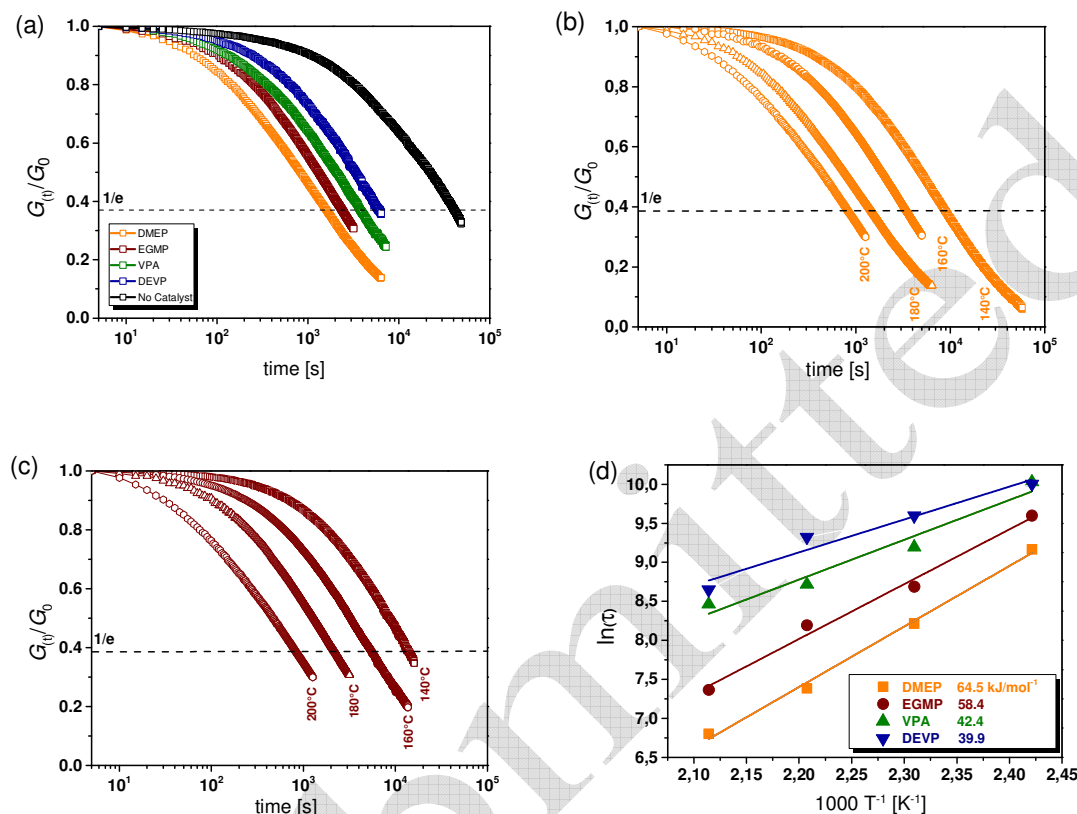


Figure 3. (a) Normalised stress relaxation curves of catalysed and non-catalysed thiol-acrylate networks obtained at 180 °C. Normalised stress relaxation curves of (b) DMEP and (c) EGMP catalysed thiol-acrylate network obtained at 140, 160, 180 and 200 °C. (d) Arrhenius plots of catalysed thiol-acrylate networks derived from the measured relaxation times.

Interestingly, the non-protic and nearly neutral dialkyl alkylphosphonate DEVP is also able to accelerate transesterifications in thiol-acrylate photopolymers, albeit at a lower rate than the protic catalysts. We assume that the compound contains not fully esterified by-products, whose –OH groups might be able to efficiently catalyse transesterifications. This is also confirmed by the FTIR spectrum of neat DEVP revealing a distinctive band related to –OH groups between 3693 and 3315 cm^{-1} (Figure S2 in supporting information). The presence of

acidic –OH groups would also explain the ability of the resin to undergo acid-catalysed dark reactions as the crosslink density is slightly higher than the reference system containing no catalyst (Table 1).

The stress relaxation of the four catalysed networks is clearly temperature-dependent (Figure 3b and 3c and Figure S3a and S3b in supporting information) and characteristic for dynamic networks, in which the bond exchange rate increases with rising temperature.^[2]

In vitrimers, the relaxation time (τ^*) follows an Arrhenius-type temperature dependency $\tau^* = \tau_0 \exp(E_a/RT)$, in which E_a corresponds to the activation energy and R is the universal gas constant.^[6,18] According to the Maxwell Model, τ^* can be derived from the measured relaxation data by taking the normalized relaxation modulus ($G(t)/G_0$) required to relax e^{-1} (37%) of the initial stress.^[6] In Figure 3c, τ^* is plotted against $(1/T)$ in a semilogarithmic scale and the linear trend obtained for all four catalysed systems confirms the Arrhenius-type temperature dependence and the vitrimeric nature of the network.^[7,30]

The activation energy (E_a) of the catalysed networks was determined, by taking the slope ($m=E_a/R$) of the straight line fitted to the data. The results reveal that vitrimers catalysed with stronger Brønsted acids have higher E_a values, which indicates a higher temperature-dependency of the networks' exchange kinetics. The same trend was also found by Bates et al. in low-Tg polyester networks at temperatures between 25 and 60 °C.^[22] By using strong Brønsted acids with pKa values ranging from – 12 to 0.81, they were able to obtain E_a values between 49.6 and 66.7 kJ mol⁻¹. It is interesting to note that in the thiol-acrylate vitrimers under investigation, the relaxation times and their temperature dependence can be adjusted over a similar range (42.4 – 64.5 kJ mol⁻¹), with protic catalysts spanning a narrower range of pKa values (1.29 – 2.11). For DEVP, the lowest E_a value is obtained (39.9 kJ mol⁻¹), which is explained by the low acidity of the dialkyl alkylphosphonate.

From the results it can be concluded that the exchange reactions in thiol-acrylate vitrimers are very sensitive to the acidity of the phosphate or phosphonate catalyst with stronger Brønsted

acids giving rise to higher E_a values and faster relaxation rates. The difference in the exchange kinetics also directly affects the T_v , at which the network changes from a viscoelastic solid to a viscoelastic liquid.^[17] The T_v values were derived by extrapolation of the fitted data to a relaxation time of 10^6 s and are given in Table 1. The T_v data correlate well with the pKa value of the catalysts and the E_a values of the related dynamic networks and gradually increases from 49 to 59 °C. The results clearly show that organic phosphates and phosphonates are versatile catalysts in accelerating dynamic exchange reactions in vitrimeric photopolymers and based on their acidity enable a convenient tuning of exchange kinetics and T_v . In addition, Brønsted acids exhibit a better performance in catalysing transesterifications in vitrimers compared to Lewis acid catalysts such as $Zn(OAc)_2$.^[22] Whilst lower crosslinked acrylate networks with $Zn(OAc)_2$ require 120 min (at 180 °C) to relax 63% of the initial stress, the DMEP catalysed thiol-acrylate is nearly ten times faster (15 min) under the same conditions.^[15] Even in the DEVP-catalysed network the initial stress is being relaxed within shorter time (102 min) giving rise to the superior activity of organic phosphates and phosphonates in thiol-click vitrimers relying on transesterifications.

3. Conclusion

In this study, organic phosphates and phosphonates were exploited to catalyse reversible transesterifications in photocurable thiol-click vitrimers. The low- T_g networks were highly mobile at elevated temperature and facilitated bond exchange reactions, whose rate was sensitive to the acidity of the applied catalyst. E_a values and relaxation rate increased with increasing pKa value of the catalyst giving rise to a higher temperature-dependency of the networks' exchange kinetics. Along with exchange kinetics, the acidity of the catalyst directly affected the T_v , which increased from 49 to 59 °C. The study further revealed that protic organic phosphates are superior in catalysing dynamic exchange reactions in vitrimeric

photopolymers. In particular, DMEP catalysed networks are up to 10 times faster to relax stresses at a given temperature compared to vitrimers containing typical Lewis acids.

4. Experimental Part

4.1 Materials and chemicals

Ethylene glycol methacrylate phosphate (EGMP) containing up to 25% of diester, was supplied by Gute Chemie, Germany. Vinyl phosphonic acid (VPA), diethyl vinyl phosphonate (DEVP) and Sudan II were purchased from Tokyo Chemical Industry Co., Japan.

Trimethylolpropane tri(3-mercaptopropionate) was obtained from Bruno Bock Chemische Fabrik GmbH & Co. KG, Germany. All other chemicals, including bis (2-methacryloyloxy ethyl) phosphate (DMEP), 2-hydroxy-2-phenoxypropyl acrylate, glycerol 1,3-diclycerolate diacrylate, phenylbis(2,4,6-trimethylbenzoyl) phosphine oxide were purchased from Sigma-Aldrich and used as received.

4.2 Sample preparation

2-hydroxy-3-phenoxy propyl acrylate (50 mol%) was added to glycerol 1,3-diclycerolate diacrylate (25 mol%) in a light-protected vessel along with one of the catalysts (3.75 mol% related to –OH groups) and mixed. 0.05 wt% Sudan II was added, and the formulation underwent ultra-sonication until the dissolution of the photo-absorber. The mixtures were then supplemented with 2 wt% phenylbis(2,4,6-trimethylbenzoyl) phosphine oxide and 25 mol% trimethylolpropane tri(3-mercaptopropionate) and were stirred at 100 rpm at room temperature. Accordingly, four formulations were prepared, and for each formulation, one of the catalysts (ethylene glycol methacrylate phosphate, bis (2-methacryloyloxy ethyl phosphate), vinyl phosphonic acid, or diethyl vinyl phosphonate) was used. In addition, one formulation was prepared without a catalyst as a reference.

4.3 Characterisation of cure kinetics and network properties

A Vertex 70 FTIR spectrometer (Bruker, USA) was used to follow the curing process induced by light. Sixteen scans were collected in transmission mode between 4000 and 700 cm^{-1} with a resolution of 4 cm^{-1} , and the measurement of the absorption peak area was facilitated using OPUS software. 1.5 μL of each resin formulation was drop cast between two CaF_2 discs, and curing was carried out by a light-emitting diode lamp (zgood[®] wireless LED curing lamp), which led to a power density of 3.3 mW cm^{-2} ($\lambda = 420 - 450 \text{ nm}$). The curing process was followed up to 600 s light exposure until the characteristic carbonyl and thiol peaks ceased to change in intensity. The conversion rates were calculated from the normalized intensity of C=C and S-H peaks using OPUS software.

Stress relaxation analysis was carried out in a moving die rheometer (Anton Paar, Austria) at 140, 160, 180 and 200 $^{\circ}\text{C}$. Prior to measurement, the specimens were equilibrated at 20 N at the selected analysis temperature for 20 min. Then, a 3% step strain was applied, and the stress was recorded over-time until 37% relaxation was achieved.

Dynamic Mechanical Analysis (DMA) was carried out by exploiting a dynamic mechanical analyzer (DMA/SDTA861e, Mettler-Toledo GmbH, Switzerland) on samples with the width of 4.5 mm, and a thickness of 1 mm with a clamping distance of 10.5 mm in tensile mode. The scans were performed between -20 and 90 $^{\circ}\text{C}$ using a heating rate of 2 $^{\circ}\text{C}/\text{min}$ with a frequency of 1 Hz, and maximum amplitude of 10 μm .

For equilibrium swelling measurements discs with a diameter of 10 mm were 3D DLP printed and immersed in dichloromethane at 23 $^{\circ}\text{C}$ for 48 h. After the excess solvent on the surface was removed carefully using tissue paper, the weight of the swollen gel was determined. The samples were then dried at 40 $^{\circ}\text{C}$ until constant weight and reweighed to obtain the gel contents. Mass swelling ratios were determined by $(m_s - m_d)/m_d$ with m_s being the mass of the swollen sample and m_d its initial mass. Five samples were tested for each network and the arithmetic average was taken.

4.4 Bottom-up digital light processing 3D Printing

3D DLP printing was carried out using an Anycubic Photon Zero printer (China) supplied with a LED 405 nm light source. Two bottom layers were exposed for 20 s, while the other layers were irradiated for 8 s. The circular specimens were set to be prepared with a height of 50 μm using a building speed of 3 mm s^{-1} , and a retracting speed of 3 mm s^{-1} . To carry out the post-curing process, specimens were heated at 60 $^{\circ}\text{C}$ for 20 min in an oven. Then, the curing was completed by subsequent UV irradiation using microwave-powered UV-lamp with dichroic reflector, constant UV-emission, bulb length of 250 mm, and a power of 249 W cm^{-1} .

Supporting Information

Supporting Information is available from the Wiley Online Library or from the author.

Acknowledgements

Part of the research work was performed with the “SMART” project. This project has received funding from the European Union’s Horizon 2020 research and innovation programme under the Marie Skłodowska-Curie grant agreement No 860108.

Part of the research work was performed also within the COMET-Module “Chemitecture” (project-no.: 21647048) at the Polymer Competence Center Leoben GmbH (PCCL, Austria) within the framework of the COMET-program of the Federal Ministry for Transport, Innovation and Technology and the Federal Ministry for Digital and Economic Affairs with contributions by the Institute of Chemistry of Polymeric Materials (Montanuniversitaet Leoben, Austria). The PCCL is funded by the Austrian Government and the State Governments of Styria, Upper and Lower Austria.

Received: ((will be filled in by the editorial staff))

Revised: ((will be filled in by the editorial staff))

Published online: ((will be filled in by the editorial staff))

References

- [1] a) C. J. Kloxin, C. N. Bowman, *Chem. Soc. Rev.* **2013**, *42*, 7161; b) W. Alabiso, S. Schlögl, *Polymers*. **2020**, *12*, 1660;
- [2] J. M. Winne, L. Leibler, F. E. Du Prez, *Polym. Chem.* **2019**, *10*, 6091.
- [3] D. Montarnal, M. Capelot, F. Tournilhac, L. Leibler, *Science*. **2011**, *334*, 965.
- [4] N. J. van Zee, R. Nicolay, *Progress in Polymer Science*. **2020**, *104*, 101233.
- [5] D. Montarnal, M. Capelot, F. Tournilhac, L. Leibler, *Science (New York, N.Y.)*. **2011**, *334*, 965.
- [6] M. Capelot, M. M. Unterlass, F. Tournilhac, L. Leibler, *ACS Macro Lett.* **2012**, *1*, 789.
- [7] W. Denissen, J. M. Winne, F. E. Du Prez, *Chemical science*. **2016**, *7*, 30.
- [8] F. I. Altuna, C. E. Hoppe, R. J.J. Williams, *European Polymer Journal*. **2019**, *113*, 297.
- [9] X. Niu, F. Wang, X. Li, R. Zhang, Q. Wu, P. Sun, *Ind. Eng. Chem. Res.* **2019**, *58*, 5698.

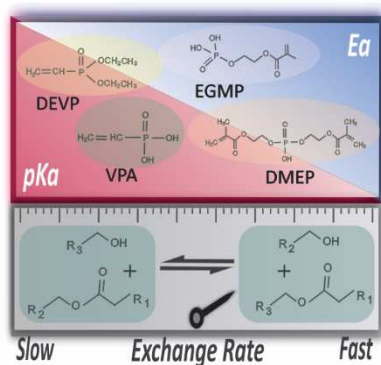
- [10] A. Demongeot, S. J. Mougner, S. Okada, C. Soulié-Ziakovic, F. Tournilhac, *Polym. Chem.* **2016**, *7*, 4486.
- [11] Z. Tang, Y. Liu, B. Guo, L. Zhang, *Macromolecules.* **2017**, *50*, 7584.
- [12] L. Cao, J. Fan, J. Huang, Y. Chen, *J. Mater. Chem. A.* **2019**, *167*, 421.
- [13] A. Legrand, C. Soulié-Ziakovic, *Macromolecules.* **2016**, *49*, 5893.
- [14] Z. Feng, J. Hu, H. Zuo, N. Ning, L. Zhang, B. Yu, M. Tian, *ACS Appl. Mater. Interfaces.* **2018**, *11*, 1469.
- [15] B. Zhang, K. Kowsari, A. Serjouei, M. L. Dunn, Q. Ge, *Nature communications.* **2018**, *9*, 1831.
- [16] Y. Yang, Z. Pei, X. Zhang, L. Tao, Y. Wei, Y. Ji, *Chem. Sci.* **2014**, *5*, 3486.
- [17] Z. Yang, Q. Wang, T. Wang, *ACS applied materials & interfaces.* **2016**, *8*, 21691.
- [18] a) S. Kaiser, S. Wurzer, G. Pilz, W. Kern, S. Schlögl, *Soft Matter.* **2019**, *15*, 6062; b) S. Kaiser, J. N. Jandl, P. Novak, S. Schlögl, *Soft Matter.* **2020**;
- [19] G. B. Lyon, L. M. Cox, J. T. Goodrich, A. D. Baranek, Y. Ding, C. N. Bowman, *Macromolecules.* **2016**, *49*, 8905.
- [20] E. Rossegger, R. Höller, D. Reisinger, J. Strasser, M. Fleisch, T. Griesser, S. Schlögl, *Polym. Chem.* **2021**, *117*, 10212.
- [21] a) E. Lotero, Y. Liu, D. E. Lopez, K. Suwannakarn, D. A. Bruce, J. G. Goodwin, *Ind. Eng. Chem. Res.* **2005**, *44*, 5353; b) P. A. Alaba, Y. M. Sani, W. M. Ashri Wan Daud, *RSC Adv.* **2016**, *6*, 78351;
- [22] J. L. Self, N. D. Dolinski, M. S. Zayas, J. Read de Alaniz, C. M. Bates, *ACS Macro Lett.* **2018**, *7*, 817.
- [23] a) F. Bazi, H. El Badaoui, S. Sokori, S. Tamani, M. Hamza, S. Boulaajaj, S. Sebti, *Synthetic Communications.* **2006**, *36*, 1585; b) K. Thinnakorn, J. Tscheikuna, *Applied Catalysis A: General.* **2014**, *476*, 26;
- [24] E. M. Arnett, G. W. Mach, *J. Am. Chem. Soc.* **1966**, *88*, 1177.
- [25] A. Farahi, F. Bentiss, C. Jama, M. A. El Mhammedi, M. Bakasse, *Journal of Alloys and Compounds.* **2017**, *723*, 1032.
- [26] U. Salz, A. Mucke, J. Zimmermann, F. R. Tay, D. H. Pashley, *The Journal of Adhesive Dentistry.* **2006**, *8*, 3, 143.
- [27] B. Danko, A. W. Trochimczuk, Z. Samczyński, A. Hamerska-Dudra, R. S. Dybczyński, *Reactive and Functional Polymers.* **2007**, *67*, 1651.
- [28] L. Macarie, G. Iliu, *Progress in Polymer Science.* **2010**, *35*, 1078.
- [29] B. Bingöl, W. H. Meyer, M. Wagner, G. Wegner, *Macromol. Rapid Commun.* **2006**, *27*, 1719.
- [30] D. H. Ripin, D. A. Evans, *pKa's of inorganic and oxoacids*, 206th edition. **2005**.
- [31] L. Imbernon, S. Norvez, L. Leibler, *Macromolecules.* **2016**, *49*, 2172.
- [32] C. E. Hoyle, T. Y. Lee, T. Roper, *Journal of Polymer Science Part A: Polymer Chemistry.* **2004**, *42*, 5301.
- [33] a) A. F. Senyurt, H. Wei, C. E. Hoyle, S. G. Piland, T. E. Gould, *Macromolecules.* **2007**, *40*, 4901; b) T. Y. Lee, T. M. Roper, E. S. Jonsson, C. A. Guymon, C. E. Hoyle, *Macromolecules.* **2004**, *37*, 3606; c) S. K. Reddy, K. S. Anseth, C. N. Bowman, *Polymer.* **2005**, *46*, 4212; d) Melahat Sahin, Santhosh Ayalur - Karunakaran, Jakob Manhart, Markus Wolfahrt, Wolfgang Kern, Sandra Schlögl, *Advanced Engineering Materials.* **2017**, *19*, 1600620;
- [34] B. P. Sutherland, M. Kabra, C. J. Kloxin, *Polym. Chem.* **2021**, *38*, 646.
- [35] J. Chen, S. Jiang, Y. Gao, F. Sun, *J Mater Sci.* **2018**, *53*, 16169.

The catalytic activity of organic phosphonates and phosphates is comprehensively studied in thiol-acrylate vitrimers. The strong Brønsted acids accelerate transesterifications at elevated temperature. Cure kinetics, T_g and storage modulus are not affected by the acidity of the catalysts. In contrast, pK_a values of the catalysts correlate well with T_v , relaxation times and activation energies, providing a convenient tool to control the dynamic characteristics of vitrimers.

Keyword transesterification catalysts

K. Moazzen, E. Rossegger, W. Alabiso, U. Shaukat, Dr. S. Schlögl*

Role of organic phosphates and phosphonates in catalysing dynamic exchange reactions in thiol-click vitrimers



Supporting Information

Role of organic phosphates and phosphonates in catalysing dynamic exchange reactions in thiol-click vitrimers

Khadijeh Moazzen, Elisabeth Rossegger, Walter Alabiso, Usman Shaukat and Sandra Schlögl*

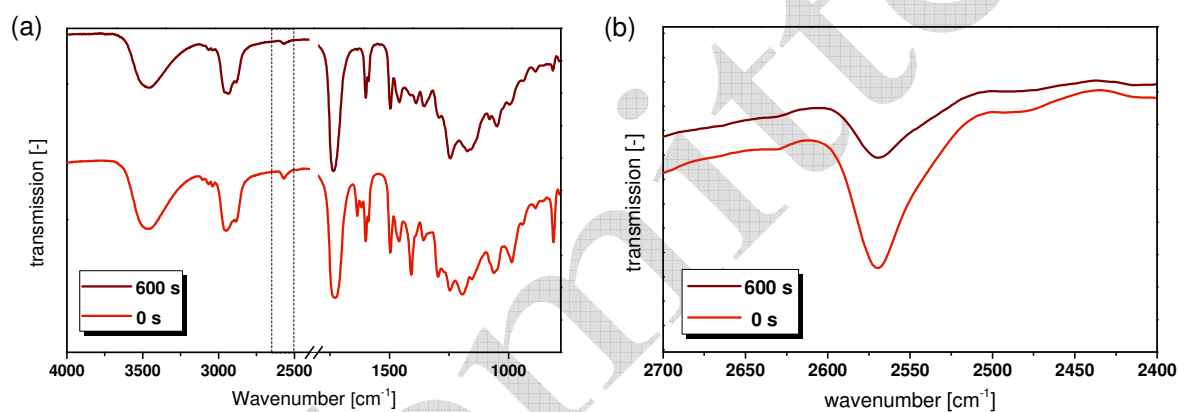
1. Results and Discussion*1.1 Curing kinetics and FTIR spectrum of DEVP*

Figure S1. (a) FTIR spectra of DMEP-catalysed thiol-acrylate network prior to and after photocuring ($\lambda = 420 - 450 \text{ nm}$, 3.3 mW cm^{-2}) under air. (b) IR bands of the characteristic thiol groups magnified out of the FTIR spectra.

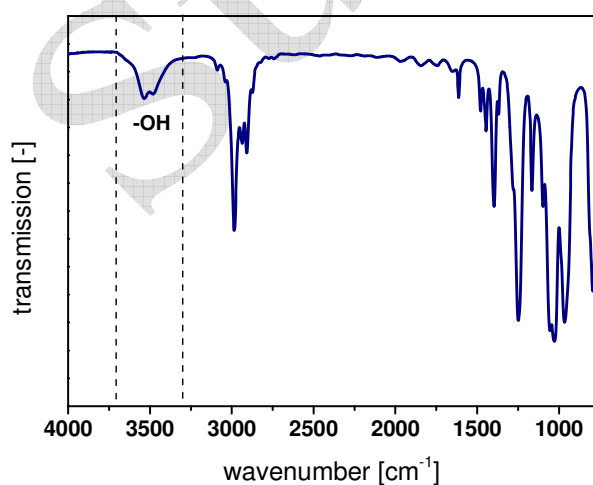


Figure S2. FTIR spectrum of neat DEVP

1.2 Stress relaxation experiments

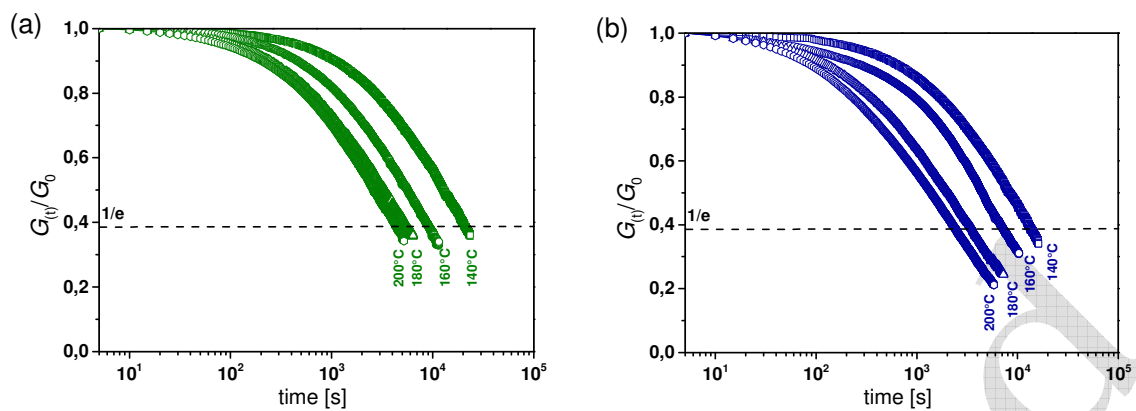


Figure S3. (a) Normalised stress relaxation curves of the VPA catalysed thiol-acrylate network obtained at 140, 160, 180 and 200 °C. (b) Normalised stress relaxation curves of the DEVP catalysed thiol-acrylate network obtained at 140, 160, 180 and 200 °C.